J. Phys. Res. Edu., Vol. 2, March 2025

Effect of Core and Its Position on the Properties of Fluorinated Nematic Liquid Crystals

Biplab Kumar Singha, Ashim Debnath, and Sripada Haldar*

Department of Physics, University of North Bengal,

Raja Ramohunpur, 734013, Darjeeling, India

Five nematic liquid crystal (NLC) compounds have been investigated by polarizing optical microscopy (POM), molecular mechanics and dielectric spectroscopy. Introduction of ethane (–CH_2CH_2–) bridge, its position, surrounding rings and fluorination were found to influence considerably molecular dipole moment (μ), inclination (β) i.e., frame of reference, dielectric anisotropy ($\Delta\varepsilon$), threshold voltage (V_{th}), splay elastic constant (K_{11}), relaxation time (τ) and activation energy (E_a). It is observed that compounds show very lower melting and clearing temperatures. Nematic (N) phase stability is also found to be broader. All compounds show super cooling property near to room temperature except compound 3o2pp-f (N1). Splay elastic constant (K_{11}), an important parameter is found to vary from 10^{-11} N to 10^{-10} N. Comparatively lower value of K_{11}, lower value of restoring torque and alternatively faster response can be achieved. Undesirable energy absorption is found in between few hundred kHz to MHz region i.e flip-flop in nature.

I. INTRODUCTION

Liquid crystal (LC) is a distinct phase of matter observed between the crystalline solid and isotropic liquid states that can flow as an isotropic liquid while exhibiting crystalline solids like anisotropic properties [1–7]. Many of the distinctive fascinating behaviors of LCs make them growing in using widely in display devices. Liquid crystal displays (LCDs) are still dominating till date most commonly in market over other displays. LCDs are commonly used in calculators, digital wristwatches, digital cameras, mobile phones, E-books, video players, pc monitors, televisions, laboratory instrument panels, aircraft cockpit panels, etc [8–10]. LCs are also widely used in non-display technology in addition to the display technology such as spatial light modulators, optical light valves, micro-color filters, tunable color filters, tunable wave-plates, lenses, telecommunications switching, optical recognition, optical computing, etc [11–16]. However, it is impossible for a single LC to satisfy all the properties required necessarily for practical applications. To meet the different criterion for applications, structural changes have been made by varying rings, functional groups, linkage between rings and position of the core, etc. We have investigated five fluorinated nematic LCs. Chemical structures of them differ from each other due to positional difference of the ethane ($-CH_2CH_2-$) bridge, fluorination and surrounding rings of the bridge. The most common features among

the samples are fluoro-substituted terminal group, $-C_3H_7$ alkyl chain except for N_4 ($-C_5H_7$), and presence of ethane ($-CH_2CH_2-$). The presence of ethane bridge has a great tendency to form broad nematic phase than the samples having $-CH{=}CH-$ and $-C{\equiv}C-$ bridge although thermal efficiency plays opposite role [17]. The fluoro substituted terminal is capable of lowering clearing point more than cyano and isothiocyanato terminal although viscoelastic coefficient is quite higher than cyano and isothiocyanato terminated compounds [3, 6, 18–23].

The aim for the selection of these compounds is to investigate qualitatively the impact of bridge position, surrounding rings, incorporation i.e. fluorinated polar terminal group near the vicinity of the core or away from the core, and to predict so far the correlation between the comprising units of the molecule with positional changes of the bridge together with the others functional changes. In view of the application in day-to-day life for domestic and commercial utilities, melting point and clearing point of the compounds plays a big role. The compounds selected for our study come out to be of lower melting point, a reasonable clearing point and more interestingly exhibit super cooling property near to room temperature except N1 (discussed in next part). Dielectric spectroscopy is a well-studied method to understand the associated rotational dynamics of the molecules in LCs and the various factors that affect the dielectric properties are rigidity and flexibility of the molecule, polarity, length of terminal group(s), longitudinal to transverse dimensional ratio, position of dipole moment relative to principal molecular axis, rotational freedom, arrangement of the molecule and the thermodynamic environment [24, 25]. We have investigated five fluoro-terminated compounds by POM, molecular mechanics and dielectric study and a comprehensive comparative study thereafter has been made between them.

II. EXPERIMENTAL

Molecular structures and transition temperatures of the investigated compounds with their symbolic names are presented in Table I. Transition temperatures of the compounds were determined by POM study with the help of a polarizing optical microscope (Model: BX41, Olympus Corporation, Tokyo, Japan) equipped with a CCD camera (Moticam 2500, Motic Scientific, Schertz, USA) having 5MP resolution. During this measurement, the temperatures of the samples were regulated within $\pm$ 1 °C using a Mettler FP90 central processor and FP82HT hot stage (Mettler-Toledo Ltd. Greifensee, Switzerland). Textures of the investigated compounds were taken at a magnification 20x. Dielectric cells made of low resistive ($\sim$ 20Ω/sq) transparent indium tin oxide (ITO) coated glass plates with an effective area of 1cm^2 and of thickness 5 μm were used for POM and dielectric measurements. The inner surfaces of the cell glass plates were rubbed with polyimide for homogeneous alignment (HG) of the molecules. For homeotropic (HT)

molecular alignment we applied a DC electric field of 5V/μm across the HG cell. Cells were filled with the compounds in the isotropic phase by capillary action and cooled down very slowly to get proper alignment for the dielectric study. Dielectric measurement was carried out using a HIOKI 3532-50 impedance analyzer (40Hz-5MHz) (Model: 3532-50, Hoiki E.E. Corporation, Koizumi, Japan). During this measurement temperature of the samples were regulated by the same temperature controller and hot stage as described in POM study. The characteristic dielectric parameters such as the dielectric increment ($\Delta\varepsilon$) and the relaxation frequency (f_R) were extracted by representing the dielectric spectra with the following modified Cole-Cole function [26, 27].

$$\varepsilon^* = \varepsilon' - j\varepsilon'' = \varepsilon_\infty + \frac{\Delta\varepsilon}{1 + (j\frac{f}{f_R})^{1-\alpha}} - j\frac{\sigma_i}{2\pi\epsilon_0}\left(\frac{1}{f}\right)^m - jAf^n, \tag{1}$$

where α is the symmetric distribution parameter whose value lies in between 0 to 1 ($\alpha = 0$ representing Debye type behavior), f_R is the relaxation frequency and $\Delta\varepsilon$ is the dielectric increment which is the difference between the low (ε_0) and high (ε_∞) frequency limit permittivities. ϵ_0 is the free space dielectric permittivity. The third and the fourth terms are to account for the low frequency ionic conductance and the high frequency ITO resistance. σ_i, m, A and n are fitting parameters.

III. RESULTS AND DISCUSSIONS

A. POM study

The phase transition temperature of the compounds obtained from POM study during heating and cooling are listed in Table I. Highest melting temperature is found for **N1** but that for **N4**, is found to be the lowest. It is evident from Table I that the melting and clearing temperatures are found to be comparable to each other as because of structural similarities among the compounds. The molecular structures of **N2** and **N3** are quite similar i.e. same alkyl chain length and the position of $-CH_2CH_2-$ bridge except the presence of an extra fluorine atom at position 3 in ring C of **N3** (ring A, B and C is labeled in Fig. 1). For **N1**, the position of $-CH_2CH_2-$ bridge is away from the polar fluoro-substituted terminal same as **N2** and **N3** but $-CH_2CH_2-$ bridge is surrounded by bicyclooctane-benzene rings whereas the $-CH_2CH_2-$ bridge of **N2** and **N3** is surrounded by cyclohexyl-cyclohexyl rings. The position of $-CH_2CH_2-$ bridge in **N4** and **N5** is away from non-polar alkyl chain $-C_5H_{11}$ (**N4**) and $-C_3H_7$ (**N5**), reverse to that of **N1**-**N3** i.e. near to fluoro-substituted terminal and surrounded by benzene-benzene and cyclohexyl-benzene rings respectively. Thus, the position of $-CH_2CH_2-$ bridge and surrounding rings plays an important role for the alteration of melting and clearing temperatures in addition to the fluoro substitution which is also an important way in changing the melting and clearing temperatures. When the bi-cyclooctane-benzene rings

Compounds	Acronym	Structure and transition temperatures
N1	**3o2pp-f**	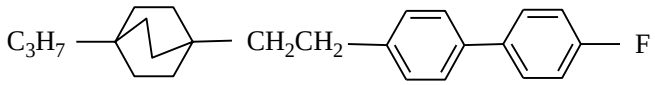 Cr 99.7 N 188 Iso
N2	**3c2cp-f**	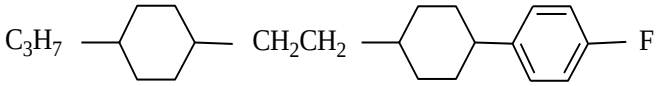 Cr 60.3 N 129 Iso
N3	**3c2cp-ff**	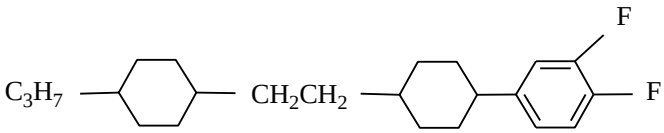 Cr 33 N 102 Iso
N4	**5cp2p-f**	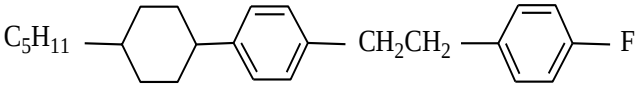 Cr 56 N 78 Iso
N5	**3cc2p-ff**	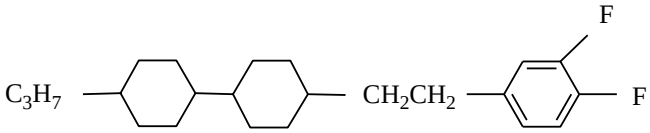 Cr38 Sm 49 N 117 Iso

TABLE I. Molecular structures of the compounds with their acronyms and phase transition temperatures (°C).

N1) of $-CH_2CH_2-$ bridge is replaced by cyclohexyl-cyclohexyl rings (**N2**), melting and clearing temperatures are found to decrease by 39.4 °C and 59 °C respectively. An extra fluorine at position 3 in ring C of **N2** when added, results **N2**$\rightarrow$ **N3** and again the melting and clearing temperatures fall by 27.3 °C and 27 °C, respectively with respect to **N2**. When $-CH_2CH_2-$ bridge is made to shift from cyclohexyl-cyclohexyl rings (**N3**) to cyclohexyl-benzene rings (**N5**) near to fluoro substitution, melting and clearing temperatures increase by 5 °C and 15 °C, respectively. The alkyl chain of **N4** is elongated by two extra carbon atoms as compared to **N1**-**N3**, **N5** and $-CH_2CH_2-$ bridge is surrounded by benzene-benzene rings, the clearing temperature of **N4** is found to be lowest (78 °C) among the investigated compounds. Thus, the position of $-CH_2CH_2-$ bridge plays a vital role in lowering the melting and clearing temperatures when surrounded by alike rings such as benzene-benzene and cyclohexyl-cyclohexyl rings. It is worth to mention here that the $-CH_2CH_2-$ bridge causes lowering of melting and clearing temperature more when surrounded by benzene-benzene rather than surrounded by cyclohexyl-cyclohexyl rings [27–29]. However, in the same

Compound	Dipole moment				Dihedral angle	β
	μ_x	μ_y	μ_z	μ		
N1	2.73	-0.39	-0.22	2.77	179°	9.7°
N2	2.62	-0.09	-0.36	2.65	175°	8.3°
N3	3.94	-1.60	0.04	4.26	175°	22.1°
N4	2.64	-0.08	-0.37	2.67	179.9°	8.6°
ISSN : 3049-026X (Online) **N5**	3.82	1.69	0.16	4.18	177.8°	23.9°

TABLE II. Molecular dipole moments with components, dihedral angle of the planes of the rings between alkyl chain and acetylene bridge and angle of resultant dipole moment relative to x-axis(β).

manner cyclohexyl-benzene surrounded $-CH_2CH_2-$ bridge is also superior in lowering melting and clearing temperatures over bicyclooctane-benzene surrounded $-CH_2CH_2-$ bridge as observed in case of **N1** and **N5** shown in Table I. Super cooling effect is observed in all cases except **N1**. Only **N5** has Smectic B phase enrich by a span of 11 °C. The appearance of SmB phase in similar type of compounds is also reported by the authors elsewhere in [25, 30]. Nematic phase stability is found to be 88.3 °C, 69.7 °C, 89 °C, 22 °C and 68 °C in **N1**-**N5**, respectively. The compound **N3** has highest nematic range of about 89 °C and that for **N4** is 22 °C, found to be the lowest. The introduction of $-CH_2CH_2-$ bridge between rings as linkage has the benefit of lowering melting and clearing temperatures as compared to the report by the authors of our laboratory [31].

A. Geometry optimization

The structure of a molecule has a definite effect on the mesomorphic properties of a LC compound [5, 32, 33]. Structural modification of the molecule can be done just by incorporating different polar groups laterally as well as at terminal positions or changing the position of linking group between different parts of the molecule which results in a drastic change in different properties like molecular dipole moment, mesomorphic temperature range, dielectric anisotropy etc. which play a significant role on practical applications in devices [31, 34]. Keeping all these in mind, energy optimized structure of the molecules is determined by Hartee-Fock method in 3-21G basis set [35] using a commercial software. Calculated dipole moment, μ and its orientation with the long molecular axis (x-axis), β and the dihedral angle between the planes of the rings on either side of $-CH_2CH_2-$ bridge of the optimized structures are listed in Table II. Non-zero value of transverse component of dipole moment in all cases reveals that the direction of resultant dipole moment will have inclination with x-axis. The highest and lowest value of dipole moment is found to be 4.26 D and 2.65 D for N3 and N2 respectively. The dipole moment of **N1**, **N4**, and **N5** is found to be 2.77 D, 2.67 D and

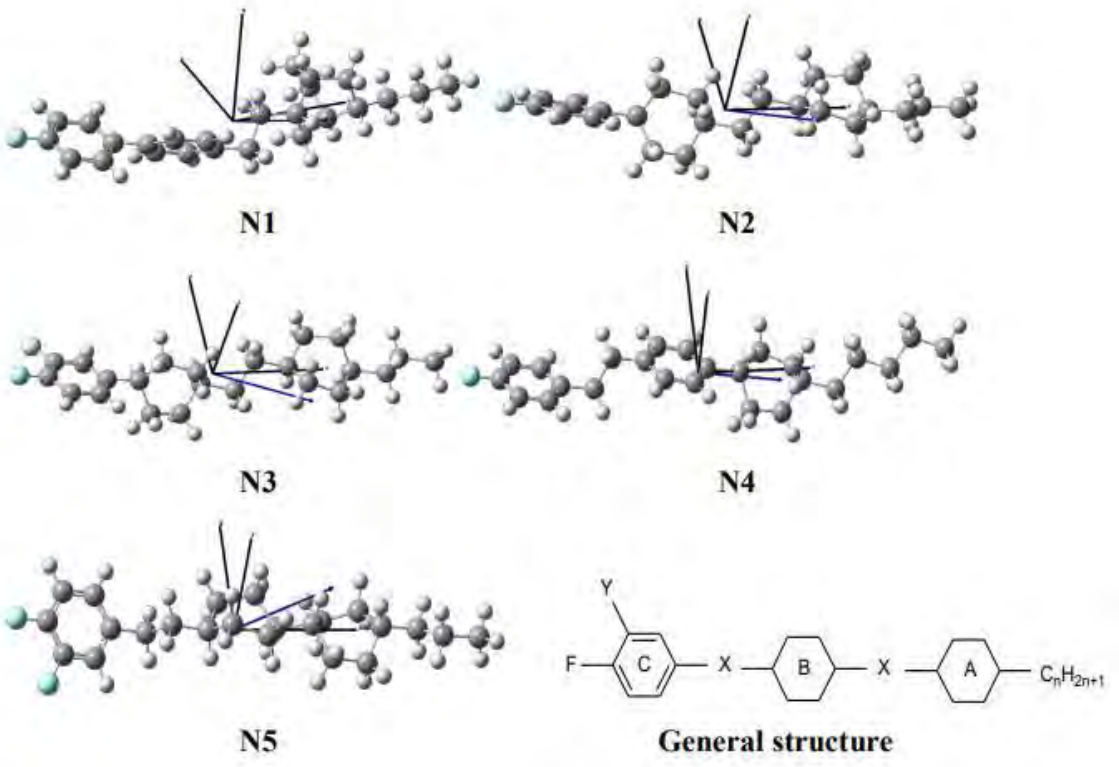

FIG. 1. Optimized molecular geometry of compound N1-N5 and general structure. (Gray: carbon; Cyan: fluorine; White: hydrogen) and general structure (X-bridge, Y-fluorine, A-cyclohexane/bi-cyclooctane, B-cyclohexane/benzene and C- benzene).

4.18 D, respectively. The dipole moment of **N3** and **N5** is almost 1.5 times the value that of **N1**, **N2**, and **N4**. Thus, doubly fluorinated **N3** and **N5** have higher value of dipole moment as compared to mono fluorinated **N1**, **N2**, and **N4**. The dihedral angle between the planes of the rings on either side of $-CH_2CH_2-$ bridge of **N2** and **N3** is found to be same 175°. It has 179°, 179.9° and 177.8° in case of **N1**, **N4**, and **N5** respectively. Therefore, a change in the reference frame has been observed when $-CH_2CH_2-$ bridge is surrounded by cyclohexyl-benzene and benzene-benzene rings unlike the cases cyclohexyl-cyclohexyl rings [25]. The higher value of dihedral angle is found for the cases when $-CH_2CH_2-$ bridge is near the fluoro-substituted terminal ($\sim$179°) than cases away from fluoro-substitution ($\sim$175°). It is worth to mention here that the introduction of $-CH_2CH_2-$ bridge changes the reference frame of the molecule [20, 25].

B. Static dielectric permittivity

From application point of view switching of the LC molecules that is the change in orientations of the molecules with respect to the applied electric field is very crucial [36, 37]. To observe the switching

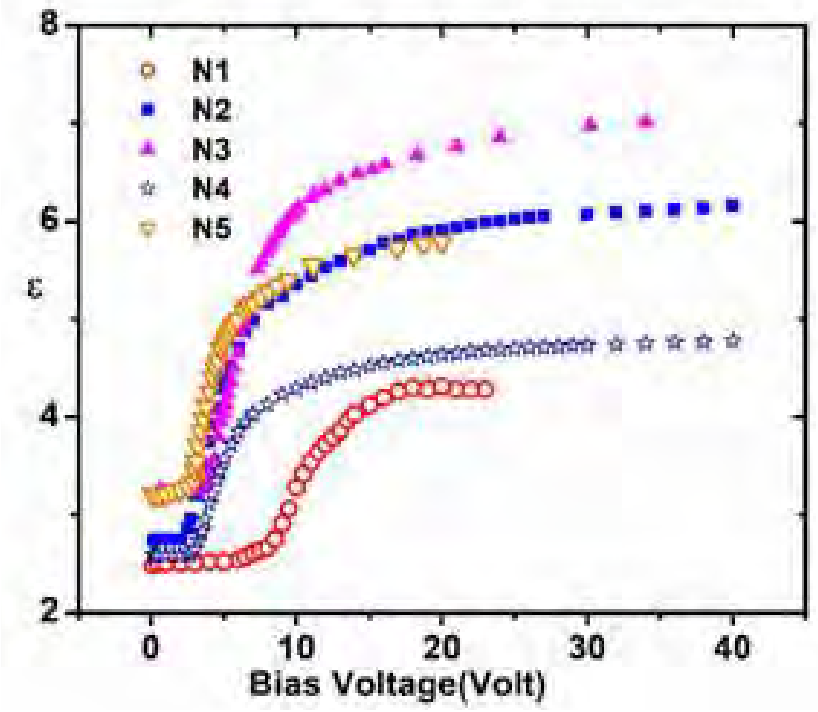

FIG. 2. Voltage dependence of real part (ε) of dielectric permittivity obtained at 10 kHz for **N1**-**N5**.

characteristics of the molecules in nematic phase, a DC electric field is applied across the homogeneous (HG) LC cell and increased gradually to get the homeotropic (HT) alignment of the molecules. From the permittivity-bias voltage graph, obtained at a fixed frequency 10 kHz shown in Fig. 2, threshold voltages (V_{th}) and driving voltages (V_d) were determined. V_{th} and V_d, respectively are the voltages at which 10% increase of the permittivity value from its minimum and 90% of the maximum permittivity were obtained [33, 38]. Threshold voltages of the investigated compounds are 8.3, 2.8, 4.4, 3.5, and 3.1 Volt, respectively.

From the values it is clear that the threshold voltages required to switch the molecules are different for different compounds. The required threshold voltage for **N1** is 8.3 Volt, found to be highest. The required threshold voltage of **N2** (2.8 volt) and N3 (4.4 volt) has almost 3- and 2-times lower than the value of **N1**. The structural difference of **N1** from **N2** is only the $-CH_2CH_2-$ bridge surrounded by bi-cyclo octane-benzene rings unlike **N2**, where the $-CH_2CH_2-$ bridge is surrounded by cyclohexyl-cyclohexyl rings. In addition to **N2**, an extra fluorine near fluorinated terminal differs **N3** from **N1**. Although di-fluorinated **N3** has slightly higher threshold voltage (4.4 V) compared to the mono-fluorinated **N2** (2.8V). Thus, fluorination enhances the required threshold voltage. The threshold voltage of **N4** and **N5** are found to be 3.5 volt and 3.1 volt, respectively. The compound **N4** has longer chain length than di-fluorinated **N5**. Thus, chain length has an impact on threshold voltages.

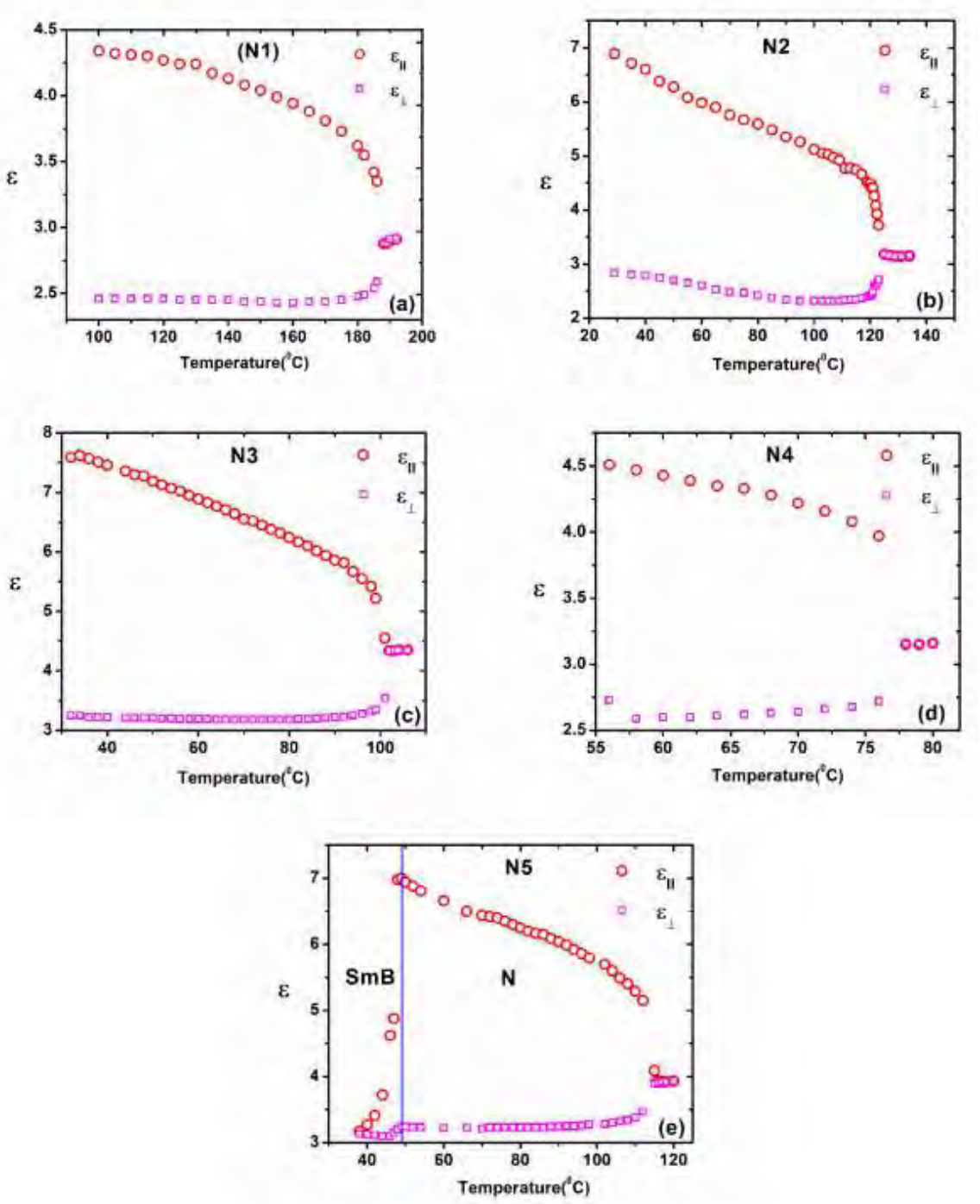

FIG. 3. Temperature dependence of parallel and perpendicular values of dielectric constants of the compounds.

From the measured values of the transverse and parallel components of dielectric constants at a fixed frequency 10 kHz, the average values of dielectric constant have been calculated using the relation $\varepsilon_{\text{avg}} = (2\varepsilon_{\perp} + \varepsilon_{\parallel})/3$ [34]. The temperature dependence of parallel and transverse values of dielectric constants for the compounds are shown in Fig. 3. Transverse component of dielectric constants remains almost constant

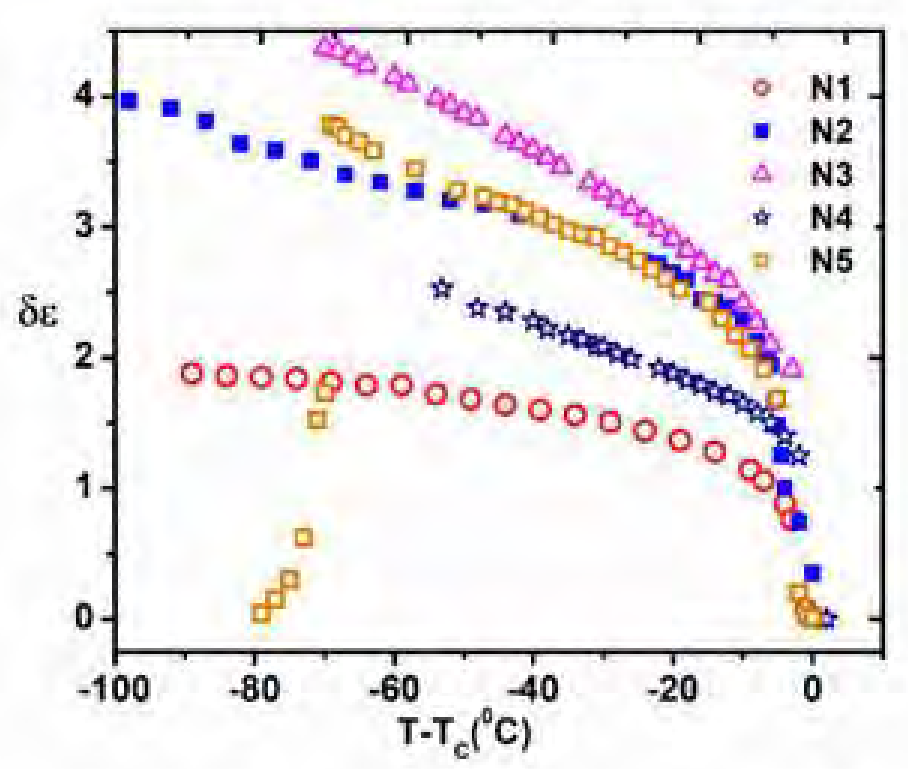

FIG. 4. Temperature dependence of dielectric anisotropy of the compounds **N1**-**N5**.

before reaching near the clearing point although a slightly higher change in values is observed in case of **N5** during SmB-N transition only due to existence of SmB phase up to 49 °C. It is worth to mention here that no such relaxation is present in HG alignment [25, 39–41]. Parallel component of dielectric constants show almost similar behavior, i.e. gradually decreasing trend with temperature except for SmB phase of **N5** where values increase faster with decrease of temperature as shown in Fig. 3 (e). The values of ε_{avg} are comparatively lower in the vicinity of N-Iso transition than ε_{Iso}. Such difference is attributed to antiparallel association of the molecules with the dipole moment in N phase [42].

Temperature variation of dielectric anisotropy ($\delta\varepsilon$) is plotted in Fig. 4. It is clear from the figure that $\delta\varepsilon$ increases with decrease in temperature in all cases except for SmB phase observed in **N5** where $\delta\varepsilon$ values decreases with decrease in temperature. $\delta\varepsilon$ values of **N1** and **N2** differ from each other although both of these are mono fluorinated and same alkyl chain length. The only difference between them in their structure is $-CH_2CH_2-$ bridge, surrounded by two different rings, bicyclooctane-benzene for **N1** and cyclohexyl-cyclohexyl for the later one. When an extra fluorine is added at position 3 in ring C of **N2** results di-fluorinated **N3** and the values of $\delta\varepsilon$ is found to be the highest. So, fluoro-substitution causes to increase $\delta\varepsilon$ [5, 18, 20, 43–45]. The $\delta\varepsilon$ value of mono fluorinated **N4** is higher than mono fluorinated **N1**

but lower than mono fluorinated **N2**. Although the increase in chain length however induces higher value in dipole moment of **N4** ($-C_5H_{11}$) in comparison with **N2** ($-C_3H_7$) but the $\delta\varepsilon$ values of **N2** still yield higher than **N4**. Values threshold voltage of **N1**, **N2** and **N4** are found to be in sequence as **N2<N4<N1** and the corresponding dipole moment values are as **N2<N4<N1** but resulted $\delta\varepsilon$ values are as **N2>N4>N1**. This is attributed due to the change incorporated by $-CH_2CH_2-$ bridge as the exchange of cyclohexyl ring on benzene/bi-cyclooctane ring enhances $\delta\varepsilon$ value in greater way [40]. So, a linear relation is found between dipole moments and threshold voltages [41–44]. When the positional change of $-CH_2CH_2-$ bridge is made in between di-fluorinated **N5** and **N3**, value of dipole moment increases from 4.18 D to 4.26 D and the corresponding value of $\delta\varepsilon$ increases 3.19 to 3.27 and from 3.58 to 3.83 at temperature 72 °C and 54 °C, respectively. So, the separation of $\delta\varepsilon$ between **N5** and **N3** increases at lower temperatures regime. Higher growth in $\delta\varepsilon$ is observed only in case of SmB phase of **N5**. Moreover, the calculated inclination β, relative to x-axis (para-axis) is found to be 22.1° and 23.9° (nearby as well) in case cases of di-fluorinated **N3** and **N5**, respectively, of the two higher $\delta\varepsilon$ valued compounds.

From the knowledge of threshold voltage and dielectric anisotropy ($\delta\varepsilon$) and using the following Freedricksz relation [Eq. (2)] [46–48], the splay elastic constant (K_{11}) can also be calculated :

$$K_{11} = \frac{\epsilon_0 \delta\varepsilon}{\pi^2} V_{\text{th}}^2, \tag{2}$$

where, ϵ_0 is the free space permittivity, $\delta\varepsilon$ is the dielectric anisotropy and V_{th} is the threshold voltage. Temperature variation of K_{11} has been shown in Fig. 5.

Splay elastic constant (K_{11}) is an important parameter to switch the molecules in nematic display devices and depends on the external applied electric field. K_{11} is also found to vary with temperature, with the increase in temperature, decrease in K_{11} obtained except SmB phase in **N5** as shown in Fig. 5. The variation of K_{11} is found to be 1.12×10^{-10} - 4.58×10^{-11} N), (2.7×10^{-11}-1.57×10^{-11} N), (7.55×10^{-11} - 3.31×10^{-11} N), (2.78×10^{-11}-1.37×10^{-11} N) and 3.28×10^{-11}-1.45×10^{-11} N (SmB: 3.44×10^{-13}-1.30×10^{-11} N) for the compounds respectively. As the values of K11 is directly proportional to square of V_{th} (equation 2), K11 is found to have in sequence with Vth except N4 only (V_{th} : **N1 > N3 > N4 > N5 > N2** and K_{11}: **N1>N3>N5>N2>N4**). Compound with higher K_{11}, higher value of V_{th} is required to switch the molecules. Compound **N4** has higher value of V_{th} compared to that of **N2** and **N5** but K_{11} is found to be lower. This may be due to the proportionate decrease in $\delta\varepsilon$ of **N4** with respect to **N2** and **N5**. This may also be due to the shortest span of mesomorphic range of **N4** (Cr 56 °C -78 °C N) as K_{11} varies with temperature inversely.

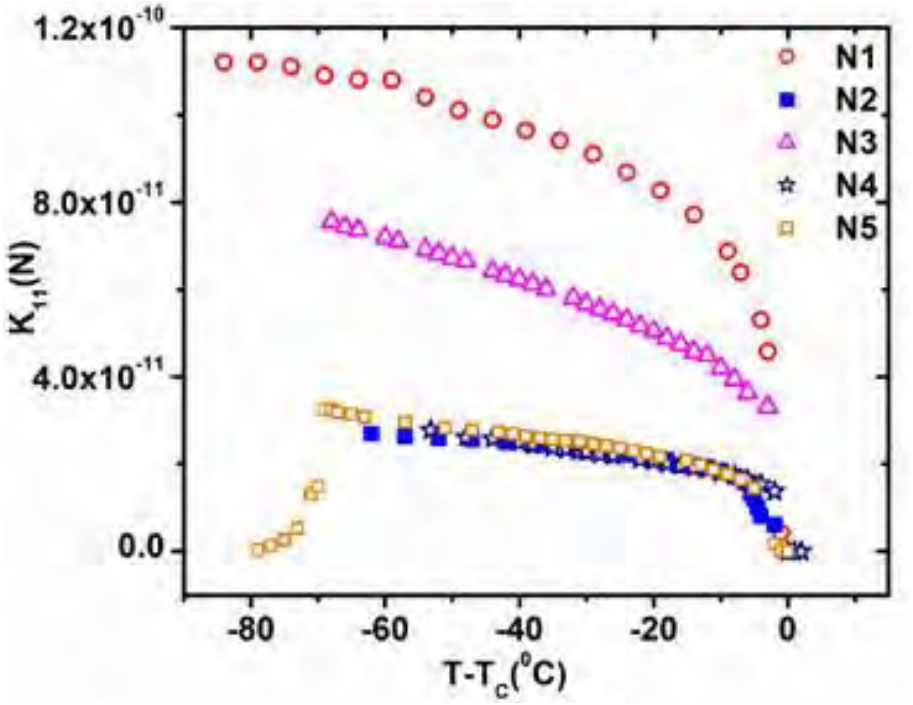

FIG. 5. Temperature dependence of splay elastic constant (K_{11}) of the compounds.

C. Dielectric relaxation study

To see the dynamic response to an applied oscillating field for the compounds, frequency dependent dielectric studies as a function of temperature were carried out in HG and HT alignment. The frequency dependent real and imaginary parts of permittivities at some selected temperatures as a representative case for the compounds are shown in Fig. 6. It is clear that the real part of complex permittivity shows almost similar, decreases very slowly in low frequency regime although in high frequency regime it decreases rapidly. It is also noticed that real part of complex permittivity of **N5** could not be aligned in SmB phase and thereby a considerable drop in permittivity is observed as shown in Fig.6 (c). A similar drop in permittivity is also observed in SmB phase by J Czub et al. [29, 49, 50]. The strength of dielectric relaxation shows a gradual decrease with temperature in N phase. Di-fluorinated **N3** and **N5** has higher dielectric loss compared to the mono fluorinated **N1**, **N2** and **N4**. All the compounds has one strong absorption process only in the measured frequency window. The range of relaxation frequencies is found to be 1.4-3.5 MHz, 0.8-4.9 MHz, 0.2-1.2MHz, 0.9-1.6 MHz and 0.9-2.5 MHz respectively. It can be highlighted here that the absorption process is associated with molecular rotation around molecular short axis.

The contributions to relaxation from other sources are limited although to some extent ionic conductivity may involve in playing a negligible role [51, 52].

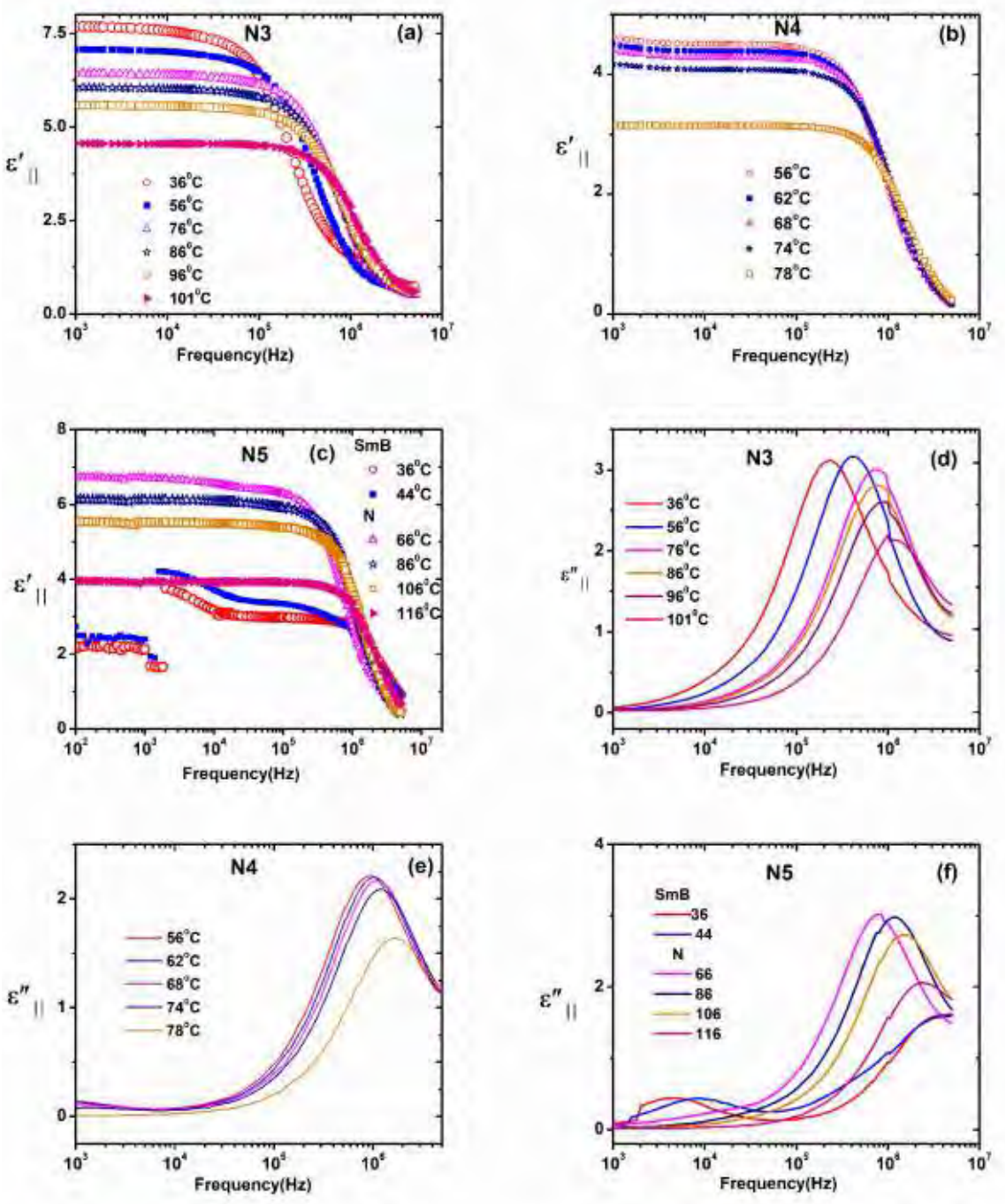

FIG. 6. Frequency dependence of real [(a), (b), and (c)] and imaginary [(d), (e), and (f)] parts of permittivity of **N3**-**N5** as representative cases at some selected temperatures in HT configuration.

As real and imaginary parts of dielectric constants are related through the Kramers-Kronig relations, the Cole-Cole plot of the fitted spectra in homeotropic alignment of N1 and N3-N5 at some selected temperatures is shown as a representative case in Fig.7. In homeotropic alignment, the Cole-Cole plots show

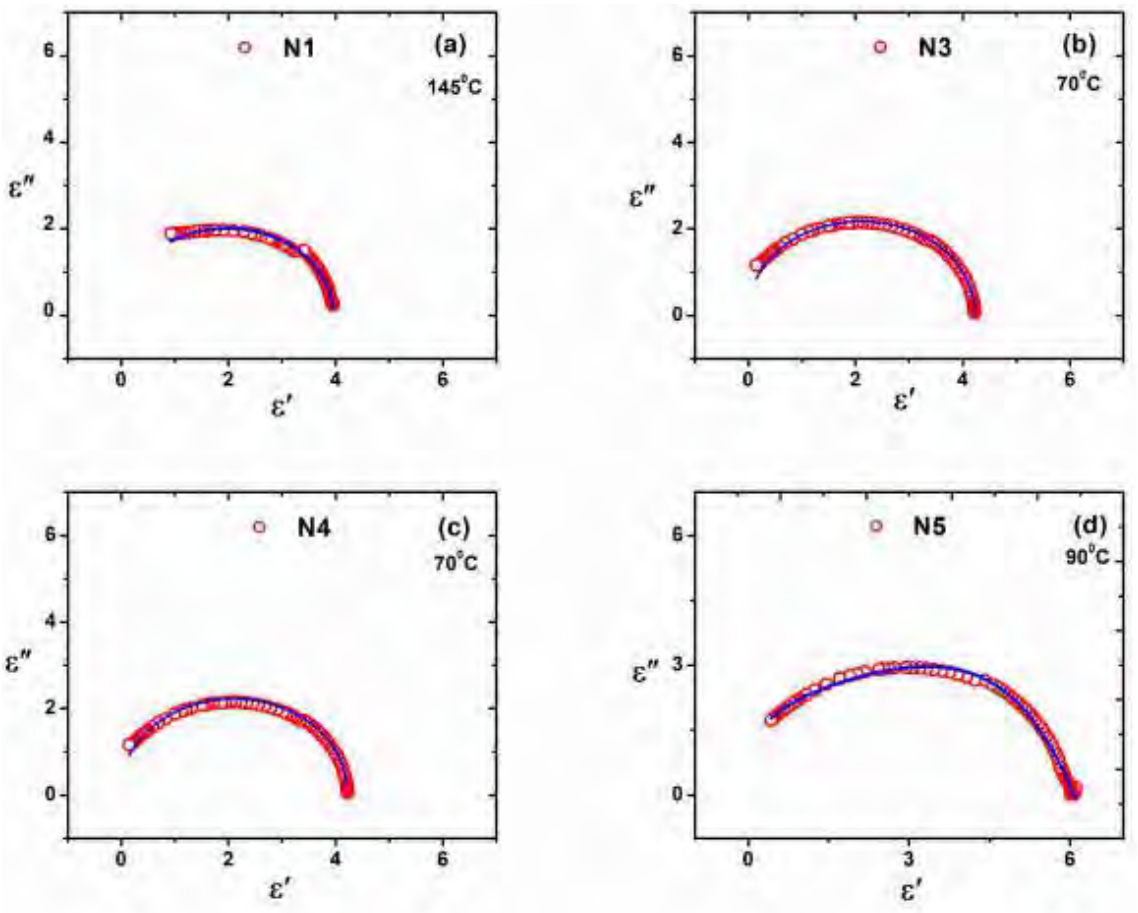

FIG. 7. Cole-Cole plots (Homeotropic alignment) of N1 and **N3**-**N5** at some selected temperatures.

almost a semi-circle (Fig.7) and the values of symmetric distribution parameter (α) is found to be very much less than 0.05 suggesting Debye type relaxation. In homeotropic alignment almost exponential increase of relaxation frequencies with temperature is observed (Fig. 8), must obey the Arrhenius law. Energy of the activation barrier is also calculated by applying Arrhenius law to the observed relaxation frequency data as shown in Fig. 9. Activation energies were found to be 28.35 kJ/mol, 24.60 kJ/mol, 21.62 kJ/mol, 12.99 kJ/mol and 21.92 kJ/mol in N phase. The value found in case of SmB phase (**N5**) is 63.99 kJ/mol, is more than 3 and 2 times greater than the value found in N phase of **N3** and **N5** respectively. A very high value of threshold voltage is required for SmB phase to switch the molecules. On fluorination at position 3 in ring C, of **N2**, **N2**$\rightarrow$ **N3**, thereby activation energy falls by an amount of 2.98 kJ/mol. Having almost same structural elements between **N2** and **N3** except an extra fluorine near the fluorinated terminal of **N3** shows fluorination(s) decrease activation energy [20, 31, 36, 53, 54]. The activation energy of mono fluorinated **N2** in which $-CH_2CH_2-$ bridge is surrounded by cyclohexyl-cyclohexyl rings is lower than **N1** by an amount of 3.75kJ/mol where $-CH_2CH_2-$ bridge is surrounded by bi-cyclooctane-benzene rings. Mono

fluorinated compound N4 has very lower activation energy, almost half of **N1** and **N2** respectively those are also mono fluorinated in nature. When the $-CH_2CH_2-$ bridge is shifted from cyclohexyl-cyclohexyl rings to in between cyclohexyl-benzene rings, although small but a decrease in activation value of 0.30 kJ/mol is observed.

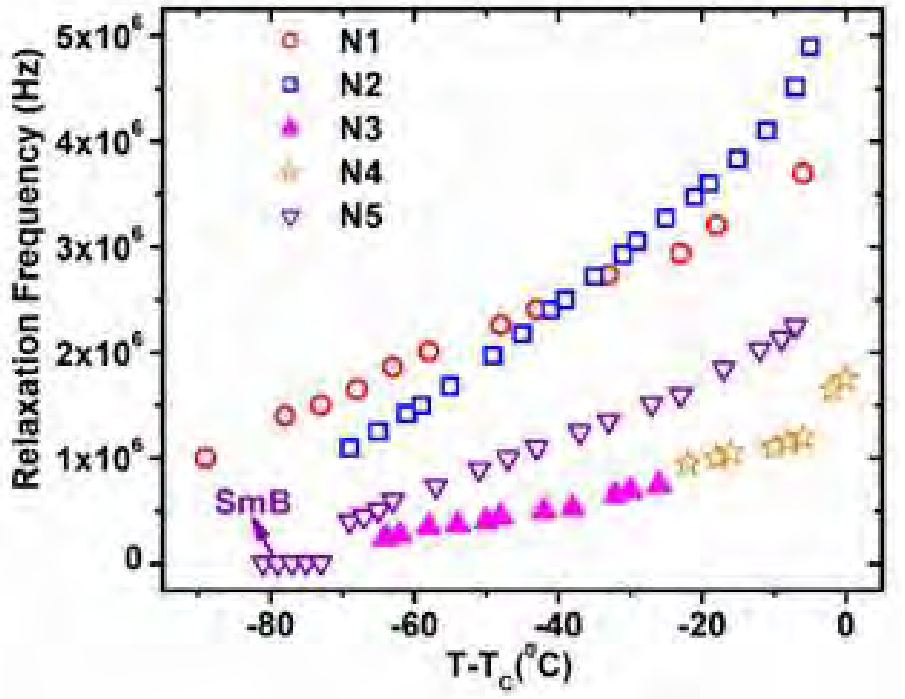

FIG. 8. Temperature dependence of relaxation frequency plots of **N1**-**N5**.

Furthermore, the activation energy of **N1**-**N5** can be arranged in descending order by **N1>N2>N5>N3>N4**, comparatively smaller value of Ea is calculated for **N4**, mono fluorinated one whose $-CH_2CH_2-$ bridge is surrounded by benzene-fluoro-benzene rings. So positional dependency of activation energy on $-CH_2CH_2-$ bridge is observed. The activation energy of the compounds are very much less than the activation energy for the compounds with structural similarities without $-CH_2CH_2-$ bridge as reported by Sinha et al. [54].

D. Conductivity

We have calculated the ac conductivity (σ_{ac}) using the following relations [55–58]

$$\sigma_{ac} = \epsilon_0 \omega \varepsilon'' \tag{3}$$

and

$$\sigma_{ac} = \sigma_{dc} + A\omega^n, \tag{4}$$

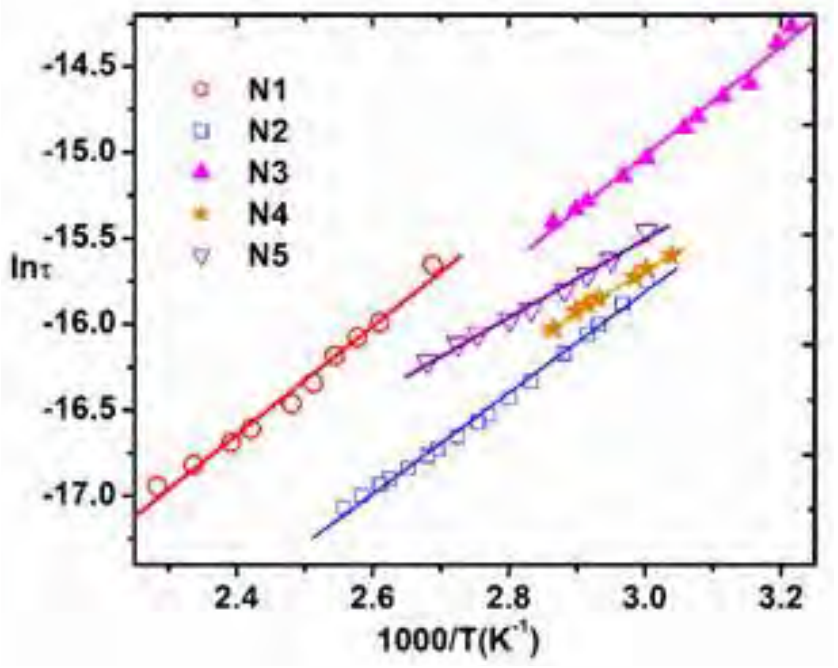

FIG. 9. Arrhenius plots in Nematic phase of the compounds **N1**-**N5**.

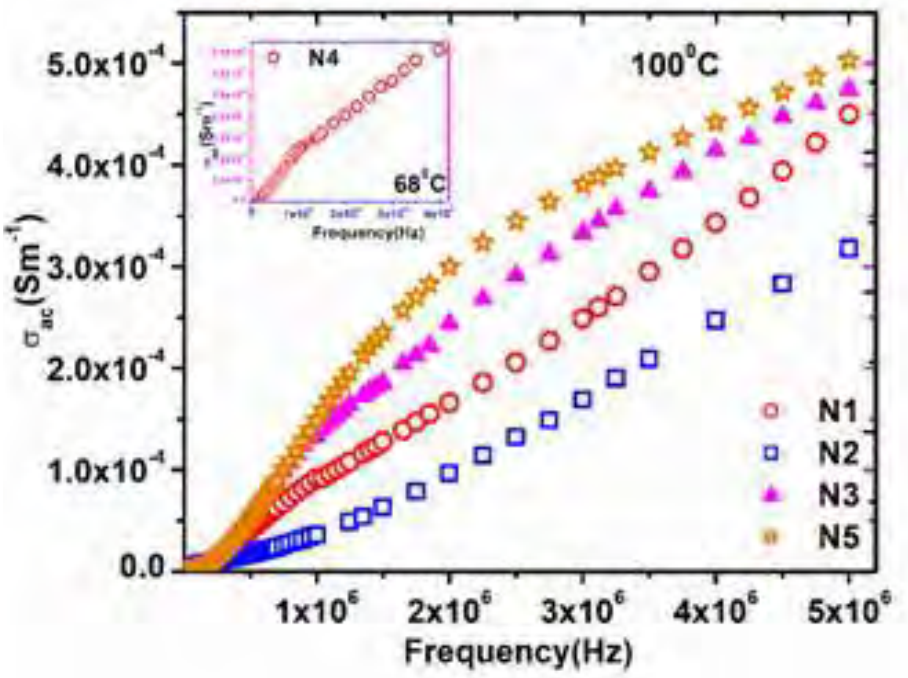

FIG. 10. Frequency variation of ac conductivity of the compounds.

where, $\omega = 2\pi f$, f is the linear frequency and A is the temperature dependent pre-exponential factor and 'n' is the frequency exponent. The variation of σ_{ac} with frequency at some particular temperatures is shown in

Fig.10. For **N1**-**N3** and **N5** at 100 °C that of **N4** at 68 °C because the clearing temperature is very much less than 100 °C. It is well known that the conduction process in LCs is a combination of hopping, transportation and mobilization of the charge carriers of the compounds. At low frequency regime, frequency independent like behavior is observed in all cases, may be due to random diffusion of ionic charge carriers via their activated hopping. As frequency increases, σ_{ac} found to increase but the rate of increment is different for different compounds. It is found maximum for **N5** and minimum for **N2**. The di-fluorinated **N3** and **N5** have higher values of σ_{ac} over the mono fluorinated **N1**, **N2** and **N4** as shown in Fig.10. The value of σ_{ac} of N4 lies in between of **N1** and **N2**. The range of variation of σ_{ac} is found to be very wide from $\sim 10^{-10}$ to 10^{-4} Sm^{-1} throughout the measured frequency window.

IV. CONCLUSION

A broader mesomorphic range of Nematic phase is observed for the compounds. The higher value of dihedral angle is found for the cases when $-CH_2CH_2-$ bridge is near the fluoro-substituted terminal than the cases away from fluoro-substitution. The fluorination enhances the required threshold voltage. Chain length has also an impact on threshold voltages. The incorporation of $-CH_2CH_2-$ bridge and its immediate surrounding rings plays a significant role in changing threshold voltage, dielectric anisotropy $\delta\varepsilon$, elastic constant and conductivity. Molecular dynamics study reveals the fact that molecular rotation associated is flip-flop i.e. around short molecular axis in nature obeys Debye process. Enhancement in $\delta\varepsilon$ has been observed higher in di-fluorinated compounds compared to that of the mono-fluorinated compounds. Higher values of K_{11} are observed in mono-fluorinated than the di-fluorinated compounds. Comparatively faster switching may be found in di-fluorinated compounds. The di-fluorinated compounds have higher values of σ_{ac} over the mono fluorinated compounds.

ACKNOWLEDGEMENTS

S. H. would like to express thanks to Prof. P. K. Mandal, Department of Physics, North Bengal University for his valuable suggestion. The authors are grateful to Prof. R. Dabrowski, Institute of Chemistry, Military University of Technology, Warsaw, Poland for supplying the compounds.

* nbushaldar@nbu.ac.in

[1] W.H. de Jeu, Physical Properties of Liquid Crystalline Materials, Gordon and Breach Science Publishers, New York (NY), 1980.

[2] G. Vertogen and W. H. de Jeu, Thermotropic Liquid crystals, Fundamentals. Springer- Verlag, Berlin, 1988.

[3] J. Sun, H. Xianyu, S. Gauza, and S. T. Wu, Liquid Crystals. **36**, 1401 (2009).

[4] C.O. Catanescu, L.C. Chien, and S. T. Wu, Molecular Crystals and Liquid Crystals **411**, 93 (2004).

[5] J. Dziaduszek, R. Dąbrowski, S. Urban, K. Garbat, A. Glushchenko, and K. Czupryński, Liquid Crystals. **44**, 1277 (2017).

[6] S. T. Wu and R.J. Cox, Journal of Applied Physics. **64**, 821 (1988).

[7] S. Gauza, C.H. Wen, Y. Zhao, S. T. Wu, A. Ziotek, and R. Dabrowski, Molecular Crystals and Liquid Crystals, **453**, 215 (2006).

[8] E. P. Raynes and I. C. Sage, Liquid Crystals. **42**, 722 (2015).

[9] M. Schadt, Liquid Crystals. **42**, 646 (2015).

[10] M. Schadt, LIQUID CRYSTAL MATERIALS AND LIQUID CRYSTAL DISPLAYS, 1997.

[11] S. J. Woltman, G. D. Jay, and G. P. Crawford, Liquid-crystal materials find a new order in biomedical applications, 2007.

[12] J. P. F. Lagerwall and G. Scalia, Current Applied Physics. **12**, 1387 (2012).

[13] P. Yaghmaee, O. H. Karabey, B. Bates, C. Fumeaux, and R. Jakoby, International Journal of Antennas and Propagation. **2013**, 824214 (2013).

[14] D. Ye, S. Q. Wu, Y. Yu, L. Liu, X. P. Lu, and Y. Wu, Appl. Phys. Lett. **104**, 103105 (2014).

[15] Y. Garbovskiy and I. Glushchenko, Crystals (Basel). **5**, 501 (2015).

[16] I. Abdulhalim, G. Moddel, and K. M. Johnson, Appl. Phys. Lett. **55**, 1603 (1989).

[17] M. Petrzilka, Molecular Crystals and Liquid Crystals. **111**, 329 (1984).

[18] D. Sinha, P. K. Mandal, and R. Dabrowski, Physica B: Condensed Matter. **441**, 100 (2014).

[19] D. Sinha, P. K. Mandal, and R. Dabrowski, Phase Transitions. **88** 153 (2015).

[20] R. Dabrowski, P. Kula, and J. Herman, Crystals (Basel). **3**, 443 (2013).

[21] Y. Liu, H. Ma, H. Xu, J. Sun, and K. Han, International Journal of Quantum Chemistry. **102**, 415 (2005).

[22] T. K. Devi, B. Choudhury, A. Bhattacharjee, and R. Dabrowski, Opto-Electron. Rev. **22**, 24 (2014).

[23] Y. Dai, L. Gao, Y. Chang, Z. Li, M. Cai, X. Wang, H. Xing, J. Zhu, and W. Ye, Liquid Crystals. **46**, 930 (2019).

[24] S. Patari and A. Nath, Journal of Molecular Liquids. **230**, 247 (2017).

[25] J. Czub, S. Urban, M. Geppi, A. Marini, and R. Dabrowski, Liquid Crystals **35**, 527 (2008).

[26] K. S. Cole, R. H. Cole, and J. Chem. Phys. **9**, 341 (1941).

[27] F. Gouda, K. Skarp, and S. T. Lagerwall, Ferroelectrics, **113**, 165 (1991).

[28] R. Dabrowski, J. Dziaduszek, K. Garbat, M. Filipowicz, S. Urban, S. Gauza, and G. Sasnouski, Liquid Crystals **37**, 1529 (2010).

[29] J. Czub, R. Dabrowski, J. Dziaduszek, and S. Urban, Liquid Crystals **36**, 521 (2009).

[30] S. Urban, J. Czub, J. Przedmojski, R. Dbrowski, and M. Geppi, Molecular Crystals and Liquid Crystals **477**, 87/[581]-100/[594], (2007).

[31] D. Sinha, S. Haldar, and P. K. Mandal, Phase Transitions **90**, 751 (2017).

[32] D. Sinha, D. Goswami, P. K. Mandal, L. Szczucinski, and R. Dabrowski, Molecular Crystals and Liquid Crystals **562**, 156 (2012).

[33] O. Catanescu, and L. C. Chien, Liquid Crystals **33**, 115 (2006).

[34] R. Chen, L. Zhao, Z. An, X. Chen, and P. Chen, Liquid Crystals. **44**, 2184 (2017).

[35] J. Herman, P. Harmata, O. Strzeżysz, M. Czerwiński, S. Urban, and P. Kula, Journal of Molecular Liquids. **267**, 511 (2018).

[36] A. Parish, S. Gauza, S. T. Wu, J. Dziaduszek, and R. Dabrowski, Molecular Crystals and Liquid Crystals. **489**, 22/[348]-39/[365] (2008).

[37] P. Kirsch, Journal of Fluorine Chemistry. **177**, 29 (2015).

[38] A. Debnath, and P. K. Mandal, Liquid Crystals. **46**, 234 (2019).

[39] D. Demus, Y. Goto, S. Sawada, E. Nakagawa, and H. Saito, Molecular Crystals and Liquid Crystals Science and Technology Section A: Molecular Crystals and Liquid Crystals. **260**, 1 (1995).

[40] J. Czub *et al*, Phase Transitions. **82**, 485 (2009).

[41] B. M. Andrews, G. W. Gray, and M. J. Bradshaw, Molecular Crystals and Liquid Crystals **123**, 257 (1985).

[42] J. Jadzyn, G. Czechowski, B. Zywucki, C. Legrand, P. Bonnet, and R. Dąbrowski, Zeitschrift fur Naturforschung A **48**, 871 (1993).

[43] S. Gauza, A. Parish, S. T. Wu, A. Spadlo, and R. Dabrowski, Liquid Crystals. **35**, 483 (2008).

[44] S. Gauza, A. Parish, S. T. Wu, A. Spado, and R. Dabrowski, Molecular Crystals and Liquid Crystals. **489**, 135/[461]-147/[473] (2008).

[45] M. Klasen, M. Bremer, K. Tarumi, I. K. Huh, Y. B. Kim, J. Xu, H. Okada, and S. Sugimori, al -, cite this article: Melanie Klasen et al, 1998.

[46] A. J. Seed, K. J. Toyne, J. W. Goodby, and M. Hird, Journal of Materials Chemistry. **10**, 2069 (2000).

[47] M. Hird, Chemical Society Reviews. **36**, 2070 (2007).

[48] M. Hird, Liquid Crystals. **38**, 1467 (2011).

[49] S. Urban, J. Czub, J. Przedmojski, R. Dbrowski, and M. Geppi, Molecular Crystals and Liquid Crystals. **477**, 87/[581]-100/[594] (2007).

[50] J. Czub *et al*, Liquid Crystals. **35**, 527 (2008).

[51] Y. Goto, T. Ogawa, S. Sawada, and S. Sugimori, Molecular Crystals and Liquid Crystals **209**, 1 (1991).

[52] D. Demus, Y. Goto, S. Sawada, E. Nakagawa, and H. Saito, Molecular Crystals and Liquid Crystals Science and Technology Section A: Molecular Crystals and Liquid Crystals. **260**, 1 (1995).

[53] A. Parish, S. Gauza, S.T. Wu, J. Dziaduszek, and R. Dabrowski, Liquid Crystals. **35**, 79 (2008).

[54] D. Sinha, S. Haldar, and P. K. Mandal, Phase Transitions **90**, 751 (2017).

[55] A. K. Jonscher, Nature. **267**, 673 (1977).

[56] S. Banerjee and A. Kumar, J. Appl. Phys. **109**, 114313 (2011).

[57] S. L. Srivastava and R. Dhar, Molecular Crystals and Liquid Crystals Science and Technology Section A: Molecular Crystals and Liquid Crystals **317**, 23 (1998).

[58] S. K. Prasad, M. V. Kumar, T. Shilpa, and C. V. Yelamaggad, RSC Advances **4**, 4453 (2014).